

## Preface to the Third Edition

Laser Spectroscopy continues to develop and expand rapidly. Many new ideas and recent realizations of new techniques based on old ideas have contributed to the progress in this field since the last edition of this textbook appeared. In order to keep up with these developments it was therefore necessary to include at least some of these new techniques in the third edition.

There are, firstly, the improvement of frequency-doubling techniques in external cavities, the realization of more reliable cw-parametric oscillators with large output power, and the development of tunable narrow-band UV sources, which have expanded the possible applications of coherent light sources in molecular spectroscopy. Furthermore, new sensitive detection techniques for the analysis of small molecular concentrations or for the measurement of weak transitions, such as overtone transitions in molecules, could be realized. Examples are Cavity Ringdown Spectroscopy, which allows the measurement of absolute absorption coefficients with great sensitivity or specific modulation techniques that push the minimum detectable absorption coefficient down to  $10^{-14} \text{ cm}^{-1}$ !

The most impressive progress has been achieved in the development of tunable femtosecond and subfemtosecond lasers, which can be amplified to achieve sufficiently high output powers for the generation of high harmonics with wavelengths down into the X-ray region and with pulsewidths in the attosecond range. Controlled pulse shaping by liquid crystal arrays allows coherent control of atomic and molecular excitations and in some favorable cases chemical reactions can already be influenced and controlled using these shaped pulses.

In the field of metrology a big step forward was the use of frequency combs from cw mode-locked femtosecond lasers. It is now possible to directly compare the microwave frequency of the cesium clock with optical frequencies, and it turns out that the stability and the absolute accuracy of frequency measurements in the optical range using frequency-stabilized lasers greatly surpasses that of the cesium clock. Such frequency combs also allow the synchronization of two independent femtosecond lasers.

The increasing research on laser cooling of atoms and molecules and many experiments with Bose–Einstein condensates have brought about some remarkable results and have considerably increased our knowledge about the interaction of light with matter on a microscopic scale and the interatomic interactions at very low temperatures. Also the realization of coherent matter waves (atom lasers) and investigations of interference effects between matter waves have proved fundamental aspects of quantum mechanics.

The largest expansion of laser spectroscopy can be seen in its possible and already realized applications to chemical and biological problems and its use in medicine as a diagnostic tool and for therapy. Also, for the solution of technical problems, such as surface inspections, purity checks of samples or the analysis of the chemical composition of samples, laser spectroscopy has offered new techniques.

In spite of these many new developments the representation of established fundamental aspects of laser spectroscopy and the explanation of the basic techniques are not changed in this new edition. The new developments mentioned above and also new references have been added. This, unfortunately, increases the number of pages. Since this textbook addresses beginners in this field as well as researchers who are familiar with special aspects of laser spectroscopy but want to have an overview on the whole field, the author did not want to change the concept of the textbook.

Many readers have contributed to the elimination of errors in the former edition or have made suggestions for improvements. I want to thank all of them. The author would be grateful if he receives such suggestions also for this new edition.

Many thanks go to all colleagues who gave their permission to use figures and results from their research. I thank Dr. H. Becker and T. Wilbourn for critical reading of the manuscript, Dr. H.J. Koelsch and C.-D. Bachem of Springer-Verlag for their valuable assistance during the editing process, and LE-TeX Jelonek, Schmidt and Vöckler for the setting and layout. I appreciate, that Dr. H. Lotsch, who has taken care for the foregoing editions, has supplied his computer files for this new edition. Last, but not least, I would like to thank my wife Harriet who made many efforts in order to give me the necessary time for writing this new edition.

Kaiserslautern,  
April 2002

*Wolfgang Demtröder*

## Preface to the Second Edition

During the past 14 years since the first edition of this book was published, the field of laser spectroscopy has shown a remarkable expansion. Many new spectroscopic techniques have been developed. The time resolution has reached the femtosecond scale and the frequency stability of lasers is now in the millihertz range.

In particular, the various applications of laser spectroscopy in physics, chemistry, biology, and medicine, and its contributions to the solutions of technical and environmental problems are remarkable. Therefore, a new edition of the book seemed necessary to account for at least part of these novel developments. Although it adheres to the concept of the first edition, several new spectroscopic techniques such as optothermal spectroscopy or velocity-modulation spectroscopy are added.

A whole chapter is devoted to time-resolved spectroscopy including the generation and detection of ultrashort light pulses. The principles of coherent spectroscopy, which have found widespread applications, are covered in a separate chapter. The combination of laser spectroscopy and collision physics, which has given new impetus to the study and control of chemical reactions, has deserved an extra chapter. In addition, more space has been given to optical cooling and trapping of atoms and ions.

I hope that the new edition will find a similar friendly acceptance as the first one. Of course, a textbook never is perfect but can always be improved. I, therefore, appreciate any hint to possible errors or comments concerning corrections and improvements. I will be happy if this book helps to support teaching courses on laser spectroscopy and to transfer some of the delight I have experienced during my research in this fascinating field over the last 30 years.

Many people have helped to complete this new edition. I am grateful to colleagues and friends, who have supplied figures and reprints of their work. I thank the graduate students in my group, who provided many of the examples used to illustrate the different techniques. Mrs. Wollscheid who has drawn many figures, and Mrs. Heider who typed part of the corrections. Particular thanks go to Helmut Lotsch of Springer-Verlag, who worked very hard for this book and who showed much patience with me when I often did not keep the deadlines.

Last but not least, I thank my wife Harriet who had much understanding for the many weekends lost for the family and who helped me to have sufficient time to write this extensive book.

Kaiserslautern,  
June 1995

*Wolfgang Demtröder*



## Preface to the First Edition

The impact of lasers on spectroscopy can hardly be overestimated. Lasers represent intense light sources with spectral energy densities which may exceed those of incoherent sources by several orders of magnitude. Furthermore, because of their extremely small bandwidth, single-mode lasers allow a spectral resolution which far exceeds that of conventional spectrometers. Many experiments which could not be done before the application of lasers, because of lack of intensity or insufficient resolution, are readily performed with lasers.

Now several thousands of laser lines are known which span the whole spectral range from the vacuum-ultraviolet to the far-infrared region. Of particular interest are the continuously tunable lasers which may in many cases replace wavelength-selecting elements, such as spectrometers or interferometers. In combination with optical frequency-mixing techniques such continuously tunable monochromatic coherent light sources are available at nearly any desired wavelength above 100 nm.

The high intensity and spectral monochromasy of lasers have opened a new class of spectroscopic techniques which allow investigation of the structure of atoms and molecules in much more detail. Stimulated by the variety of new experimental possibilities that lasers give to spectroscopists, very lively research activities have developed in this field, as manifested by an avalanche of publications. A good survey about recent progress in laser spectroscopy is given by the proceedings of various conferences on laser spectroscopy (see "Springer Series in Optical Sciences"), on picosecond phenomena (see "Springer Series in Chemical Physics"), and by several quasi-monographs on laser spectroscopy published in "Topics in Applied Physics".

For nonspecialists, however, or for people who are just starting in this field, it is often difficult to find from the many articles scattered over many journals a coherent representation of the basic principles of laser spectroscopy. This textbook intends to close this gap between the advanced research papers and the representation of fundamental principles and experimental techniques. It is addressed to physicists and chemists who want to study laser spectroscopy in more detail. Students who have some knowledge of atomic and molecular physics, electrodynamics, and optics should be able to follow the presentation.

The fundamental principles of lasers are covered only very briefly because many excellent textbooks on lasers already exist.

On the other hand, those characteristics of the laser that are important for its applications in spectroscopy are treated in more detail. Examples are the frequency spectrum of different types of lasers, their linewidths, amplitude and frequency stability, tunability, and tuning ranges. The optical compo-

nents such as mirrors, prisms, and gratings, and the experimental equipment of spectroscopy, for example, monochromators, interferometers, photon detectors, etc., are discussed extensively because detailed knowledge of modern spectroscopic equipment may be crucial for the successful performance of an experiment.

Each chapter gives several examples to illustrate the subject discussed. Problems at the end of each chapter may serve as a test of the reader's understanding. The literature cited for each chapter is, of course, not complete but should inspire further studies. Many subjects that could be covered only briefly in this book can be found in the references in a more detailed and often more advanced treatment. The literature selection does not represent any priority list but has didactical purposes and is intended to illustrate the subject of each chapter more thoroughly.

The spectroscopic applications of lasers covered in this book are restricted to the spectroscopy of free atoms, molecules, or ions. There exists, of course, a wide range of applications in plasma physics, solid-state physics, or fluid dynamics which are not discussed because they are beyond the scope of this book. It is hoped that this book may be of help to students and researchers. Although it is meant as an introduction to laser spectroscopy, it may also facilitate the understanding of advanced papers on special subjects in laser spectroscopy. Since laser spectroscopy is a very fascinating field of research, I would be happy if this book can transfer to the reader some of my excitement and pleasure experienced in the laboratory while looking for new lines or unexpected results.

I want to thank many people who have helped to complete this book. In particular the students in my research group who by their experimental work have contributed to many of the examples given for illustration and who have spent their time reading the galley proofs. I am grateful to colleagues from many laboratories who have supplied me with figures from their publications. Special thanks go to Mrs. Keck and Mrs. Ofiara who typed the manuscript and to Mrs. Wollscheid and Mrs. Ullmer who made the drawings. Last but not least, I would like to thank Dr. U. Hebgen, Dr. H. Lotsch, Mr. K.-H. Winter, and other coworkers of Springer-Verlag who showed much patience with a dilatory author and who tried hard to complete the book in a short time.

Kaiserslautern,  
March 1981

*Wolfgang Demtröder*

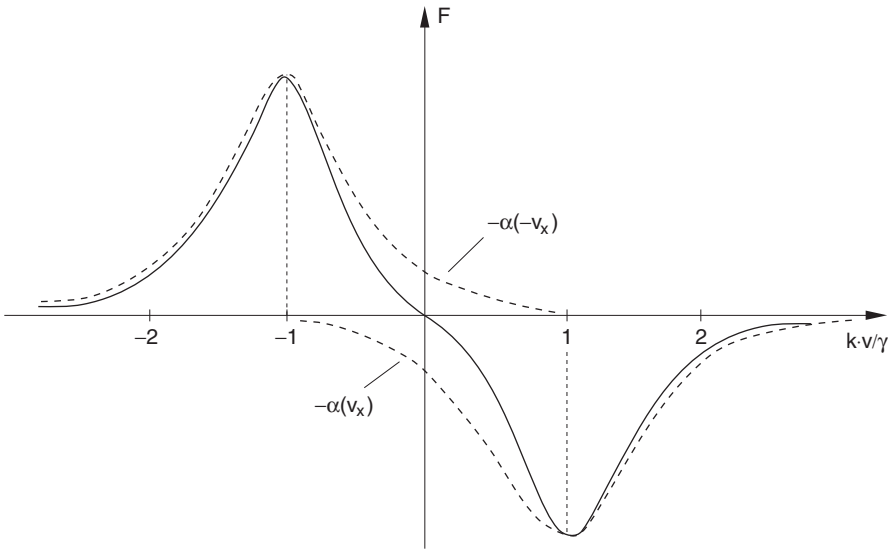


**Fig. 14.14.** Frictional force in an optical molasses (*solid curve*) for a red detuning  $\delta = -\gamma$ . The *dotted curve* shows the absorption profiles by a single atom moving with  $v_x = \pm \gamma/k$  for a single laser beam propagating into the  $x$ -direction

### Example 14.6

- (a) For rubidium atoms ( $m = 85$  AMU) the wavenumber is  $k = 8 \times 10^6 \text{ m}^{-1}$ . At a detuning  $\delta = \gamma$  and an absorption rate  $R_0 = \gamma/2$  we obtain:  $a = 4 \times 10^{-21} \text{ Ns/m}$ . This gives a damping time  $t = 35 \mu\text{s}$ .
- (b) For Na atoms with  $\delta = 2\gamma$  one obtains  $a = 1 \times 10^{-20} \text{ Ns/m}$  and  $t_D = 2.3 \mu\text{s}$ . The atoms move in this light trap like particles in viscous molasses and therefore this atomic trapping arrangement is often called *optical molasses*.

**Note:** These optical trapping methods reduce the velocity components ( $v_x$ ,  $v_y$ ,  $v_z$ ) to a small interval around  $v = 0$ . However, they do *not* compress the atoms into a spatial volume, except if the dispersion force for the field gradients  $\nabla I \neq 0$  is sufficiently strong.

### 14.1.6 Cooling of Molecules

The optical cooling techniques discussed so far are restricted to true two-level systems because the cooling cycle of induced absorption and spontaneous emission has to be performed many times before the atoms come to rest. In molecules the fluorescence from the upper excited level generally ends in

many rotational–vibrational levels in the electronic ground state that differ from the initial level. Therefore most of the molecules cannot be excited again with the same laser. They are lost for further cooling cycles.

Cold molecules are very interesting for several scientific and technical applications. One example is chemical reactions initiated by collisions between cold molecules where the collision time is very long and the reaction probability might become larger by several orders of magnitude. In addition interactions of cold molecules with surfaces where the sticking coefficient will be 100% open new insights into molecule–surface interactions and reactions between cold adsorbed molecules. Finally, the possibility to reach Bose–Einstein condensation of molecular gases opens new fascinating aspects of collective molecular quantum phenomena.

There have been several proposals how molecules might be cooled in spite of the above-mentioned difficulties [14.35–14.37]. An optical version of these proposals is based on a frequency comb laser, which oscillates on many frequencies, matching the relevant frequencies of the transitions from the upper to the lower levels with the highest transition probabilities [14.37]. In this case, the molecules can be repumped into the upper level from many lower levels, thus allowing at least several pumping cycles.

A very interesting optical cooling technique starts with the selective excitation of a collision pair of cold atoms into a bound level in an upper electronic state (Fig. 14.15). While this excitation occurs at the outer turning point of the upper-state potential, a second laser dumps the excited molecule down into a low vibrational level of the electronic ground state by stimulated emission pumping (photo-induced association). In favorable cases the level  $v = 0$  can be reached. If the colliding atoms are sufficiently cold, the angular momentum of their relative movement is zero (*S*-wave scattering). Therefore the final

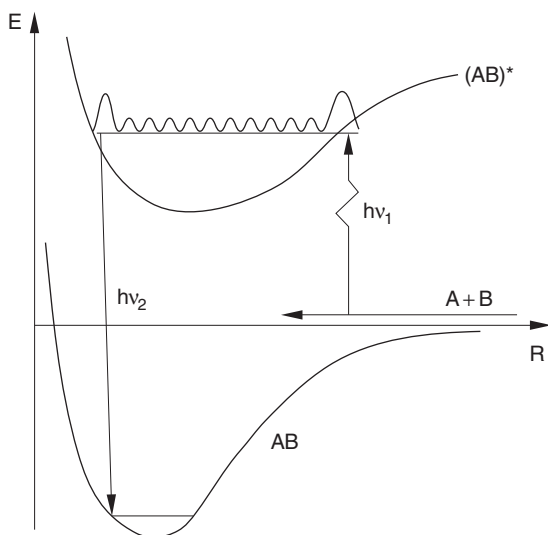


**Fig. 14.15.** Formation of cold molecules by photoassociation of a collision pair  $A+B$

ground state has the rotational quantum number  $J = 0$  if the two lasers transfer no angular momentum to the molecule (either two transitions with  $\Delta J = 0$  or the absorbing and emission transition as  $R$ -transitions with  $\Delta J = +1$  in absorption and  $-1$  in emission) [14.38].

A promising nonoptical technique relies on cooling of molecules by collisions with cold atoms. If the gas mixture of atoms and molecules can be trapped in a sufficiently small volume long enough to achieve thermal equilibrium between atoms and molecules, the optically cooled atoms act as a heat sink for the molecules, which will approach the same temperature as the atoms (sympathetic cooling) [14.39].

An interesting proposal that could be realized uses a cold supersonic molecular beam with flow velocity  $u$ , which expands through a rotating nozzle (Fig. 14.16). We saw in Chap. 9 that in supersonic beams the velocity spread around the flow velocity  $u$  may become very small. The translational temperature in the frame moving with the velocity  $u$  can be as small as 0.1 K. If the nozzle moves with the speed  $-v$ , the molecules have the velocity  $u - v$  in the laboratory frame. Tuning the angular velocity  $\omega$  of the nozzle rotating on a circle with radius  $R$  makes it possible to reach any molecular velocity  $v_m = u - \omega R$  between  $u$  and 0 in the laboratory frame. Since the beam must be collimated in order to reduce the other velocity components, there is only a small time interval per rotation period where the nozzle is in line with the collimating apertures. The cold molecules therefore appear as pulses behind the apertures.

An elegant technique has been developed in several laboratories, where cold helium clusters moving through a gas cell of atoms or molecules pick up these molecules, which then can diffuse into the interior of the helium cluster. The molecules then acquire the low temperature of the cluster. The binding energy is taken away by evaporation of He atoms from the cluster surface [14.40, 14.41].

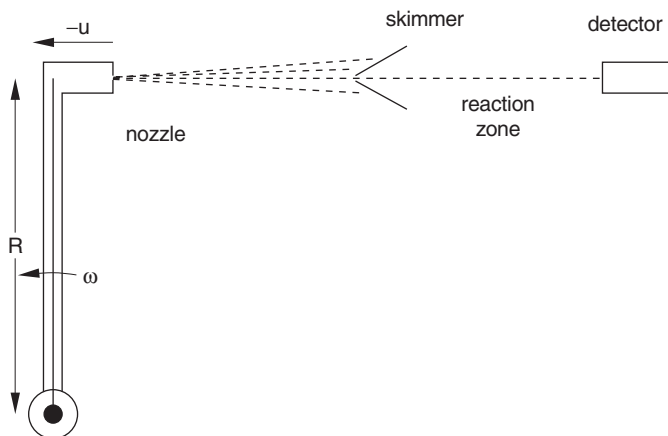


**Fig. 14.16.** Rotating nozzle for producing a beam of slow molecules

### 14.1.7 Optical Trapping of Atoms

The effectiveness of the optical molasses for cooling atoms anticipates that the atoms are trapped within the overlap region of the six laser beams for a sufficiently long time. This demands that the potential energy of the atoms shows a sufficiently deep minimum at the center of the trapping volume, that is, restoring forces must be present that will bring escaping atoms back to the center of the trapping volume.

We will briefly discuss the two most commonly used trapping arrangements. The first is based on induced electric dipole forces in inhomogeneous electric fields and the second on magnetic dipole forces in magnetic quadrupole fields. Letokhov proposed [14.42, 14.43] to use the potential minima of a three-dimensional standing optical field composed by the superposition of three perpendicular standing waves for spatial trapping of cooled atoms, whereas Ashkin and Gordon calculated [14.44] that the dispersion forces in focused Gaussian beams could be employed for trapping atoms.

#### a) Induced Dipole Forces in a Radiation Field

When an atom with the polarizability  $\alpha$  is brought into an inhomogeneous electric field  $\mathbf{E}$ , a dipole moment  $\mathbf{p} = \alpha\mathbf{E}$  is induced and the force

$$\mathbf{F} = -(\mathbf{p} \cdot \text{grad})\mathbf{E} = -\alpha(\mathbf{E} \cdot \nabla)\mathbf{E} = -\alpha[(\nabla \frac{1}{2}E^2) - \mathbf{E} \times (\nabla \times \mathbf{E})], \quad (14.23)$$

acts onto the induced dipole. The same relation holds for an atom in an optical field. However, when averaging over a cycle of the optical oscillation the last term in (14.23) vanishes, and we obtain for the mean dipole force [14.45]

$$\langle \mathbf{F}_D \rangle = -\frac{1}{2}\alpha\nabla(E^2). \quad (14.24)$$

The polarizability  $\alpha(\omega)$  depends on the frequency  $\omega$  of the optical field. It is related to the refractive index  $n(\omega)$  of a gas with the atomic density  $N$  (Sect. 3.1.3) by  $\alpha \approx \epsilon_0(\epsilon - 1)/N$ . With  $(\epsilon - 1) = n^2 - 1 \approx 2(n - 1)$  we obtain

$$\alpha(\omega) = \frac{2\epsilon_0[n(\omega) - 1]}{N}. \quad (14.25)$$

Inserting (3.37b) for  $n(\omega)$ , the polarizability  $\alpha(\omega)$  becomes

$$\alpha(\omega) = \frac{e^2}{2m_e\omega_0} \frac{\Delta\omega}{\Delta\omega^2 + (\gamma_s/2)^2}, \quad (14.26)$$

where  $m_e$  is the electron mass,  $\Delta\omega = \omega - (\omega_0 + \mathbf{k} \cdot \mathbf{v})$  is the detuning of the field frequency  $\omega$  against the Doppler-shifted eigenfrequency  $\omega_0 + \mathbf{k} \cdot \mathbf{v}$  of the atom, and  $\gamma_s = \delta\omega_n\sqrt{1+S}$  is the saturation-broadened linewidth characterized by the saturation parameter  $S$  (Sect. 3.6).

For  $\Delta\omega \ll \gamma_s$  the polarizability  $\alpha(\omega)$  increases nearly linearly with the detuning  $\Delta\omega$ . From (14.24) and (14.26) it follows that in an intense laser beam

( $S \gg 1$ ) with the intensity  $I = \epsilon_0 c E^2$  the force  $F_D$  on an induced atomic dipole is

$$\mathbf{F}_D = -a \Delta \omega \nabla I, \quad \text{with} \quad a = \frac{e^2}{m \epsilon_0 c \gamma^2 \omega_0 S}. \quad (14.27)$$

This reveals that in a homogeneous field (for example, an extended plane wave)  $\nabla I = 0$  and the dipole force becomes zero. For a Gaussian beam with the beam waist  $w$  propagating in the  $z$ -direction, the intensity  $I(r)$  in the  $x$ - $y$ -plane is, according to (5.32)

$$I(r) = I_0 e^{-2r^2/w^2}, \quad \text{with} \quad r^2 = x^2 + y^2.$$

The intensity gradient  $\nabla I = -(4r/w^2)I(r)\hat{\mathbf{r}}$  points into the radial direction and the dipole force  $\mathbf{F}_D$  is then directed toward the axis  $r = 0$  for  $\Delta \omega < 0$  and radially outwards for  $\Delta \omega > 0$ .

For  $\Delta \omega < 0$  the  $z$ -axis of an intense Gaussian laser beam with  $I(r = 0) = T_0$  represents a minimum of the potential energy

$$E_{\text{pot}} = \int_0^\infty F_D dr = +a \Delta \omega I_0, \quad (14.28)$$

where atoms with sufficiently low radial kinetic energy may be trapped. In the focus of a Gaussian beam we have an intensity gradient in the  $r$ -direction as well as in the  $z$ -direction. If the two forces are sufficiently strong, atoms can be trapped in the focal region.

Besides this dipole force in the  $r$ - and  $z$ -directions the recoil force in the  $+z$ -direction acts onto the atom (Fig. 14.17). In a standing wave in  $\pm z$ -direction the radial force and the recoil force may be sufficiently strong to trap atoms in all directions. For more details see [14.46–14.48].

### Example 14.7

In the focal plane of a Gaussian laser beam with  $P_L = 200$  mW focused down to a beam waist of  $w = 10 \mu\text{m}$  ( $I_0 = 1.2 \times 10^9$  W/m<sup>2</sup>), the radial intensity gradient is  $\partial I / \partial r = 2r/w^2 I_0 e^{-2r^2/w^2}$ , which gives for  $r = w$ :  $(\partial I / \partial r)_{r=w} = 2I_0/w \cdot e^{-2}$ . With the number above one obtains:

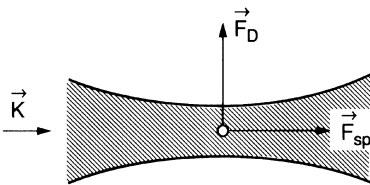


Fig. 14.17. Longitudinal and transverse forces on an atom in the focus of a Gaussian beam

$(\partial I/\partial r)_{r=w} = 2.4 \times 10^{13} \text{ W/m}^3$  and the radial dipole force acting on a Na atom is for  $\Delta\omega = -|\gamma| = -2\pi \cdot 10^7 \text{ s}^{-1}$ ,  $S = 0$ , and  $r = w$

$$F_D = +a\Delta\omega \frac{4r}{w^2} I_0 \hat{r}_0 = 1.5 \times 10^{-16} \text{ N},$$

The axial intensity gradient is for a focusing lens with  $f = 5 \text{ cm}$  and a beam diameter  $\partial I/\partial z = 4.5 \times 10^5 \text{ W/m}^3$ . This gives an axial dipole force of  $F_D(z) = 3 \times 10^{-24} \text{ N}$ , while the recoil force is about

$$F_{\text{recoil}} = 3.4 \times 10^{-20} \text{ N}.$$

In the axial direction the recoil force is many orders of magnitude larger than the axial dipole force. The potential minimum with respect to the radial dipole force is  $E_{\text{pot}} \simeq -5 \times 10^{-7} \text{ eV}$ . In order to trap atoms in this minimum their radial kinetic energy must be smaller than  $5 \times 10^{-7} \text{ eV}$ , which corresponds to the “temperature”  $T \simeq 5 \times 10^{-3} \text{ K}$ .

### Example 14.8

Assume a standing laser wave with  $\lambda = 600 \text{ nm}$ , an average intensity  $I = 10 \text{ W/cm}^2$ , and a detuning of  $\Delta\omega = \gamma = 60 \text{ MHz}$ . The maximum force acting on an atom because of the intensity gradient  $\nabla I = 6 \times 10^{11} \text{ W/m}^3$  between maxima and nodes of the field becomes, according to (14.27), with a saturation parameter  $S = 10$ :  $F_D = 10^{-17} \text{ N}$ . The trapping energy is then  $1.5 \times 10^{-5} \text{ eV} \approx T = 0.15 \text{ K}$ .

Example 14.8 demonstrates that the negative potential energy in the potential minima (the nodes of the standing wave for  $\Delta\omega > 0$ ) is very small. The atoms must be cooled to temperatures below 1 K before they can be trapped.

Another method of trapping cooled atoms is based on the net recoil force in a three-dimensional light trap, which can be realized in the overlap region of six laser beams propagating into the six directions  $\pm x, \pm y, \pm z$ .

### b) Magneto-Optical Trap

A very elegant experimental realization for cooling and trapping of atoms is the magneto-optical trap (MOT), which is based on a combination of optical molasses and an inhomogeneous magnetic quadrupole field (Fig. 14.18). Its principle can be understood as follows:

In a magnetic field the atomic energy levels  $E_i$  experience Zeeman shifts

$$\Delta E_i = -\boldsymbol{\mu}_i \cdot \mathbf{B} = -\mu_B \cdot g_F \cdot m_F \cdot B, \quad (14.29)$$

which depend on the Lande  $g$ -factor  $g_F$ , Bohr’s magneton  $\mu_B$ , the quantum number  $m_F$  of the projection of the total angular momentum  $F$  onto the field direction, and on the magnetic field  $B$ .

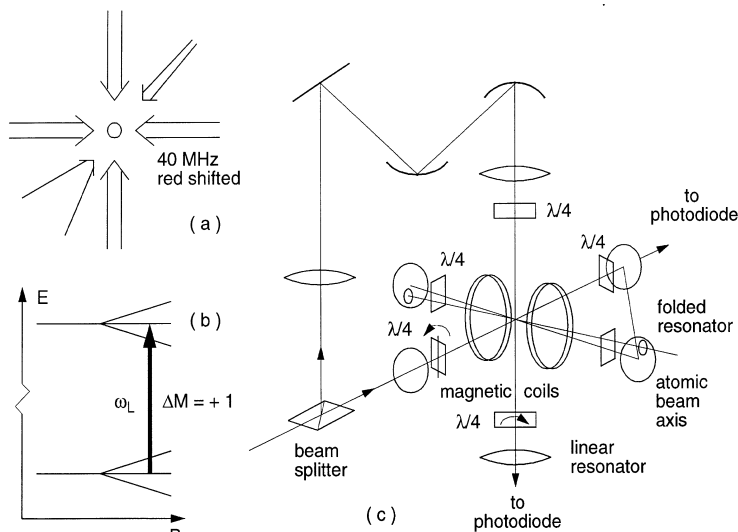


**Fig. 14.18a–c.** Realization of optical molasses [14.50a]: (a) laser beam arrangement; (b) Zeeman detuning of the  $\Delta M = +1$  transition; and (c) schematic experimental setup

In the MOT the inhomogeneous field is produced by two equal electric currents flowing into opposite directions through two coils with radius  $R$  and distance  $D = R$  (anti-Helmholtz arrangement). If we choose the  $z$ -direction as the symmetry axis through the center of the coils, the magnetic field around  $z = 0$  in the middle of the arrangement can be described by the linear dependence

$$B = bz. \quad (14.30)$$

where the constant  $b$  depends on the size of the anti-Helmholtz coils. The Zeeman splittings of the transition from  $F = 0$  to  $F = 1$  are shown in Fig. 14.18c. Atoms in the center of this MOT are exposed to the six red-tuned laserbeams of the optical molasses. Let us at first only consider the two beams in the  $\pm z$ -direction, where the laserbeam in  $+z$ -direction is  $\sigma^+$  polarized. Then the reflected beam in the  $-z$  direction is  $\sigma^-$  polarized. For an atom at  $z = 0$  where the magnetic field is zero, the absorption rates are equal for both laser beams, which means that the average momentum transferred to the atom is zero. For an atom at  $z > 0$ , however, the  $\sigma^-$ -beam is preferentially absorbed because here the frequency difference  $\omega_L - \omega_0$  is smaller than for the  $\sigma^+$ -beam. This means that the atom experiences a net momentum transfer into the  $-z$ -direction, back to the center.

In a similar way an atom at  $z < 0$  shows a preferential absorption of  $\sigma^+$ -light and gets a net momentum in the  $+z$ -direction. This shows that the atoms in the MOT are compressed toward the trap center.

We will now discuss this spatially dependent restoring force more quantitatively.

From the above discussion the net force

$$\mathbf{F}(z) = R_{\sigma^+}(z)\hbar\mathbf{k}_{\sigma^+} + R_{\sigma^-}(z)\hbar\mathbf{k}_{\sigma^-} , \quad (14.31)$$

is determined by the difference of the absorption rates  $R_{\sigma^+}$ ,  $R_{\sigma^-}$  (note that the wave vectors are antiparallel). For a Lorentzian absorption profile with halfwidth  $\gamma$ , the absorption rates become

$$R_{\sigma^\pm} = \frac{R_0}{1 + \left[ \frac{\omega_L - \omega_0 \pm \mu bz/\hbar}{\gamma/2} \right]^2} . \quad (14.32)$$

Around  $z = 0$  ( $\mu bz \ll \hbar\delta$ ) this expression can be expanded as a power series of  $\mu bz/\hbar\gamma$ .

Taking only the linear term into account yields with  $\delta = \omega_L - \omega_0$ :

$$F_z = -D \cdot z , \quad \text{with} \quad D = R_0\mu \cdot b \frac{16k \cdot \delta}{\gamma^2 (1 + (2\delta/\gamma)^2)} . \quad (14.33)$$

We therefore obtain a restoring force that increases linearly increasing with  $z$ . The potential around the center of the MOT can be then described (because of  $F_z = -\partial V/\partial z$ ) as the harmonic potential

$$V(z) = \frac{1}{2}Dz^2 . \quad (14.34)$$

The atoms oscillate like harmonic oscillators around  $z = 0$  and are spatially stabilized.

**Note:** There is a second force

$$\mathbf{F}_\mu = -\boldsymbol{\mu} \cdot \text{grad } \mathbf{B} ,$$

which acts on atoms with a magnetic moment in an inhomogeneous magnetic field.

Inserting the numbers for sodium atoms, it turns out that this force is negligibly small compared to the recoil force at laser powers in the milliwatt range. At very low temperatures, however, this force is essential to trap the atoms after the laser beams have been shut off (see Sect. 14.1.9)

In the discussion above we have neglected the velocity-dependent force in the optical molasses (Sect. 14.1.5).

The total force acting on an atom in the MOT

$$F_z = -Dz - av ,$$

results in a damped oscillation around the center with an oscillation frequency

$$\Omega_0 = \sqrt{D/m} , \quad (14.35)$$

and a damping constant

$$\beta = a/m .$$

So far we have only considered the movement in the  $z$ -direction. The anti-Helmholtz coils produce a magnetic quadrupole field with three components. From Maxwell's equation  $\text{div } \mathbf{B} = 0$  and the condition  $\partial B_x / \partial x = \partial B_y / \partial y$ , which follows from the rotational symmetry of the arrangement, we obtain the relations

$$\frac{\partial B_x}{\partial x} = \frac{\partial B_y}{\partial y} = -\frac{1}{2} \frac{\partial B_z}{\partial z} .$$

The restoring forces in the  $x$ - and  $y$ -directions are therefore half of the forces in  $z$ -directions. The trapped thermal cloud of atoms fills an ellipsoidal volume.

### Example 14.9

With a magnetic field gradient of 0.04 T/m a sodium atom at  $z = 0$  in a light trap with two counterpropagating  $\sigma^+$ -polarized laser beams  $L^+$ ,  $L^-$  in the  $\pm z$ -direction with  $I_+ = 0.8 I_{\text{sat}}$ ,  $\omega_+ = \omega_0 - \gamma/2$  and  $I_- = 0.15 I_{\text{sat}}$ ,  $\omega_- = \omega_0 + \gamma/10$ , the negative acceleration of a Na atom moving away from  $z = 0$  reaches a value of  $a = -3 \times 10^4 \text{ m/s}^2$  ( $\hat{=} 3 \times 10^3 g!$ ), driving the atom back to  $z = 0$ .

Generally, the MOT is filled by slowing down atoms in an atomic beam (see Sect. 14.1.3). Spin-polarized cold atoms can also be produced by optical pumping in a normal vapor cell and trapped in a magneto-optic trap. This was demonstrated by Wieman and coworkers [14.50b], who captured and cooled  $10^7$  Cs atoms in a low-pressure vapor cell by six orthogonal intersecting laser beams. A weak magnetic field gradient regulates the light pressure in conjunction with the detuned laser frequency to produce a damped harmonic motion of the atoms around the potential minimum. This arrangement is far simpler than an atomic beam. Effective kinetic temperatures of 1  $\mu\text{K}$  have been achieved for Cs atoms. For more details on MOT and their experimental realizations see [14.6, 14.7] and [14.51].

### 14.1.8 Optical Cooling Limits

The lowest achievable temperatures of the trapped atoms can be estimated as follows: because of the recoil effect during the absorption and emission of photons, each atom performs a statistical movement comparable to the Brownian motion. If the laser frequency  $\omega_L$  is tuned to the resonance frequency  $\omega_0$  of the atomic transition, the net damping force becomes zero. Although the time average  $\langle v \rangle$  of the atomic velocity approaches zero, the mean value of  $\langle v^2 \rangle$  increases, analogous to the random-walk problem [14.52, 14.53]. The optical cooling for  $\omega - \omega_0 < 0$  must compensate this "statistical heating" caused by the statistical photon scattering. If the velocity of the atoms has decreased

to  $v < \gamma/k$ , the detuning  $\omega - \omega_0$  of the laser frequency must be smaller than the homogeneous linewidth of the atomic transition  $\gamma$  in order to stay in resonance. This yields a lower limit of  $\hbar\Delta\omega < k_B T_{\min}$ , or with  $\Delta\omega = \gamma/2$

$$T_{\min} = \hbar\gamma/2k_B \quad (\text{Doppler limit}), \quad (14.36)$$

if the recoil energy  $E_r = \hbar\omega^2(2Mc^2)^{-1}$  is smaller than the uncertainty  $\hbar\gamma$  of the homogeneous linewidth.

### Example 14.10

- (a) For  $\text{Mg}^+$  ions with  $\tau = 2 \text{ ns} \rightarrow \gamma = 80 \text{ MHz}$  (14.36) yields  $T_{\min} = 2 \text{ mK}$ .
- (b) For Na atoms with  $\gamma = 10 \text{ MHz} \rightarrow T_{\min} = 240 \text{ }\mu\text{K}$ .
- (c) For Rb atoms with  $\gamma = 5.6 \text{ MHz} \Rightarrow T_{\min} = 140 \text{ }\mu\text{K}$ .
- (d) For Ca atoms cooled on the narrow intercombination line at  $\lambda = 657 \text{ nm}$  with  $\gamma = 20 \text{ kHz}$  the minimum temperature of  $T_{\min} = 240 \text{ nK}$  is calculated from (14.36).

Meanwhile, experiments have shown that, in fact, temperatures lower than this calculated Doppler limit can be reached [14.54–14.56]. How is this possible?

The experimental results can be explained by the following model of *polarization gradient cooling* [14.55–14.57]. If two orthogonally polarized light waves travel anticollinearly in  $\pm z$ -directions through the atoms of the optical molasses in a magnetic field, the total field amplitude acting on the atoms is

$$\mathbf{E}(z, t) = E_1 \hat{e}_x \cos(\omega t - kz) + E_2 \hat{e}_y \cos(\omega t + kz). \quad (14.37)$$

This field shows a  $z$ -dependent elliptical polarization: for  $z = 0$  it has linear polarization along the direction  $\hat{e}_1 = (\hat{e}_x + \hat{e}_y)$  (assuming  $E_1 = E_2$ ), for  $z = \lambda/8$  it has elliptical  $\sigma^-$  polarization, for  $z = \lambda/4$  again linear polarization along  $\hat{e}_2 = (\hat{e}_x - \hat{e}_y)$ , for  $z = 3\lambda/8$  elliptical  $\sigma^+$  polarization, etc. (Fig. 14.19a).

For an atom at rest with the level scheme of Fig. 14.19b, the energies and the populations of the two ground-state sublevels  $g_{-1/2}$ ,  $g_{+1/2}$  depend on the location  $z$ . For example, for  $z = \lambda/8$  the atom rests in a  $\sigma^-$  light field and is therefore optically pumped into the  $g_{-1/2}$  level, giving the stationary population probabilities  $|(g_{-1/2})|^2 = 1$  and  $|(g_{+1/2})|^2 = 0$ , while for  $z = (3/8)\lambda$  the atom is pumped by  $\sigma^+$  light into the  $g_{+1/2}$ -level.

The electric field  $\mathbf{E}(z, t)$  of the standing light wave causes a shift and broadening of the atomic Zeeman levels (*ac Stark shift*) that depends on the saturation parameter, which in turn depends on the transition probability, the polarization of  $\mathbf{E}$ , and the frequency detuning  $\omega_L - \omega_0$ . It differs for the different Zeeman transitions. Since the  $\sigma^-$  transition starting from  $g_{-1/2}$  is three times as intense as that from  $g_{+1/2}$  (Fig. 14.19b), the light shift  $\Delta_-$  of  $g_{-1/2}$  is three times the shift  $\Delta_+$  of  $g_{+1/2}$ . If the atom is moved to  $z = (3/8)\lambda$ , the situation is reversed, since now pumping occurs on a  $\sigma^+$  transition.

The  $z$ -dependent energy shift of the ground-state sublevel therefore follows the curve of Fig. 14.19c. For those  $z$  values where a linearly polarized light

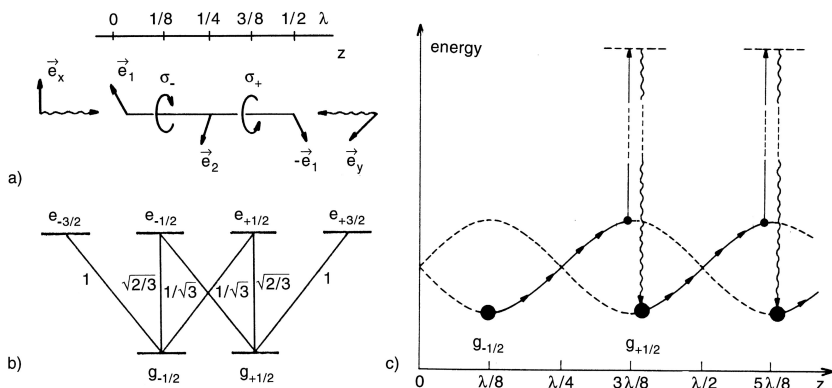


**Fig. 14.19a–c.** Schematic diagram of polarization gradient (Sisyphus) cooling: (a) two counterpropagating linearly polarized waves with orthogonal polarization create a standing wave with  $z$ -dependent polarization. (b) Atomic level scheme and Clebsch–Gordan coefficients for a  $J_g = 1/2 \leftrightarrow J_e = 3/2$  transition. (c) Atomic Sisyphus effect in the  $\text{lin} \perp \text{lin}$  configuration [14.55]

field is present, the transition probabilities and light shifts are equal for the two sublevels.

The cooling now proceeds as follows: the important point is that the optical pumping between the sublevels takes a certain time  $\tau_p$ , depending on the absorption probability and the spontaneous lifetime of the upper level. Suppose the atom starts at  $z = \lambda/8$  and moves to the right with such a velocity that it travels a distance of  $\lambda/4$  during the time  $\tau_p$ . Then it always climbs up the potential  $E_{\text{pot}}^-(g_{-1/2})$ . When the optical pumping takes place at  $t = 3\lambda/8$  (which is the maximum transition probability for  $\sigma^+$ -light!), it is transferred to the minimum  $E_{\text{pot}}^+(g_{+1/2})$  of the  $g_{+1/2}$  potential and can again climb up the potential. During the optical pumping cycle it absorbs less photon energy than it emits, and the energy difference must be supplied by its kinetic energy. This means that its velocity decreases. The process is reminiscent of the Greek myth of Sisyphus, the king of Corinth, who was punished by the gods to roll a heavy rock uphill. Just before he reached the top, the rock slipped from his grasp and he had to begin again. Sisyphus was condemned to repeat this exhausting task for eternity. Therefore polarization gradient cooling is also called *Sisyphus cooling* [14.58].

Because the population density (indicated by the magnitude of the dots in Fig. 14.19c) is larger in the minimum than in the maxima of the potentials  $E_{\text{pot}}(z)$ , on the average the atom climbs uphill more than downhill. It transfers part of its kinetic energy to photon energy and is therefore cooled.

Depending on the polarization of the two counterpropagating laser beams the  $\text{lin} \perp \text{lin}$  configuration can be used with two orthogonal linear polarizations or the  $\sigma^+ - \sigma^-$  configuration with a circularly polarized  $\sigma^+$  wave, superimposed by the reflected  $\sigma^-$  wave. With Sisyphus cooling temperatures as low as 5–10  $\mu\text{K}$  can be achieved.

### 14.1.9 Bose–Einstein Condensation

At sufficiently low temperatures where the de Broglie wavelength

$$\lambda_{\text{DB}} = \frac{h}{m \cdot v}, \quad (14.38)$$

becomes larger than the mean distance  $d = n^{-1/3}$  between the atoms in the cold gas, a phase transition takes place for bosonic particles with integer total spin. More and more particles occupy the lowest possible energy state in the trap potential and are then indistinguishable, which means that all these atoms in the same energy state are described by the same wave function (note that for bosons the Pauli exclusion principle does not apply). Such a situation of a macroscopic state occupied by many indistinguishable particles is called a *Bose–Einstein condensate* (BEC, Nobel prize in physics 2001 for E. Cornell, W. Ketterle, and C. Wiemann).

More detailed calculations show that BEC is reached if

$$n \cdot \lambda_{\text{DB}}^3 > 2.612. \quad (14.39)$$

With  $v^2 = 3k_{\text{B}}T/m$  we obtain the de Broglie wavelength

$$\lambda_{\text{DB}} = \frac{h}{\sqrt{3mK_{\text{B}}T}}, \quad (14.40)$$

and the condition (14.40) for the critical density becomes

$$n > 13.57(m \cdot k_{\text{B}}T)^{3/2}/h^3.$$

The minimum density for BEC depends on the temperature and decreases with  $T^{3/2}$  [14.6, 14.59].

#### Example 14.12

For Na atoms at a temperature of  $10 \mu\text{K}$  the critical density would be  $n = 6 \times 10^{14} / \text{cm}^3$ , which at present not achievable. For experimentally realized densities of  $10^{12} \text{cm}^{-3}$  the atoms have to be cooled below  $100 \text{nK}$  in order to reach BEC.

For rubidium atoms BEC was observed at  $T = 170 \text{nK}$  and a density of  $3 \times 10^{12} \text{cm}^{-3}$ .

### 14.1.10 Evaporative Cooling

The temperatures reached with the optical cooling methods discussed so far are not sufficiently low to obtain Bose–Einstein condensation. Here the very old and well-known technique of evaporation cooling leads to the desired goal. The principle of this method is as follows [14.60]: